# Online Appendix to
# Behavioral Learning Equilibria in the
# New Keynesian Model

Cars Hommes[a] ,   Kostas Mavromatis[b] ,   Tolga Özden[a] ,   Mei Zhu[c*]

[a] CeNDEF, School of Economics, University of Amsterdam

and Tinbergen Institute, Netherlands

[b] De Nederlandsche Bank[†]and University of Amsterdam, The Netherlands

[c] Institute for Advanced Research & School of Economics, Shanghai University of Finance and Economics,

and the Key Laboratory of Mathematical Economics(SUFE), Ministry of Education, Shanghai 200433, China

May 29, 2019

## 1 Comparison of the Fixed Point and Quasi-Newton Iterations

**Unique BLE**

This section compares the fixed point (iterative E-stability) and Quasi-Newton iterations using our benchmark calibration in Hommes et. al. (2019). The top panel of Figure 1 shows the unique BLE $\boldsymbol{\beta}^* = (\beta_y, \beta_\pi) = (0.9, 0.96)$, along with the convergence paths of the fixed point and Quasi-Newton iterations when we initialize with $\boldsymbol{\beta}^{(0)} = (0, 0)$. It is readily seen that both iteration schemes converge to the unique fixed point approximately at approximately the same speed. In order to check the sensitivity of convergence to the initial values, the following two panels in the same figure show the convergence of the fixed

---

* *E-mail addresses:* C.H.Hommes@uva.nl, K.Mavromatis@dnb.nl, T.Ozden@uva.nl Zhu.Mei@mail.shufe.edu.cn

[†]The views expressed do not represent the position of De Nederlandsche Bank or the Eurosystem.

point and Quasi-Newton iterations with randomized initial values $\boldsymbol{\beta}^{(0)} \in (0,1)^2$. Both iteration types correctly identify the unique locally stable BLE of the system regardless of the initial values, which shows that the interval $(0,1)$ is inside the basin of attraction of the equilibrium $\boldsymbol{\beta}^*$.

Figure 1: Convergence of the fixed point and Quasi-Newton iterations to the unique BLE: a graphical illustration. Top Panel: convergence when we use the initial value $\boldsymbol{\beta}^{(0)} = (0,0)$. Bottom Panels: convergence when we apply the algorithm 100 times with randomized initial values on $(0,1)^2$ using the fixed point and Quasi-Newton iterations.



**Simple Fixed Point Iteration:**



**Quasi-Newton Iteration:**
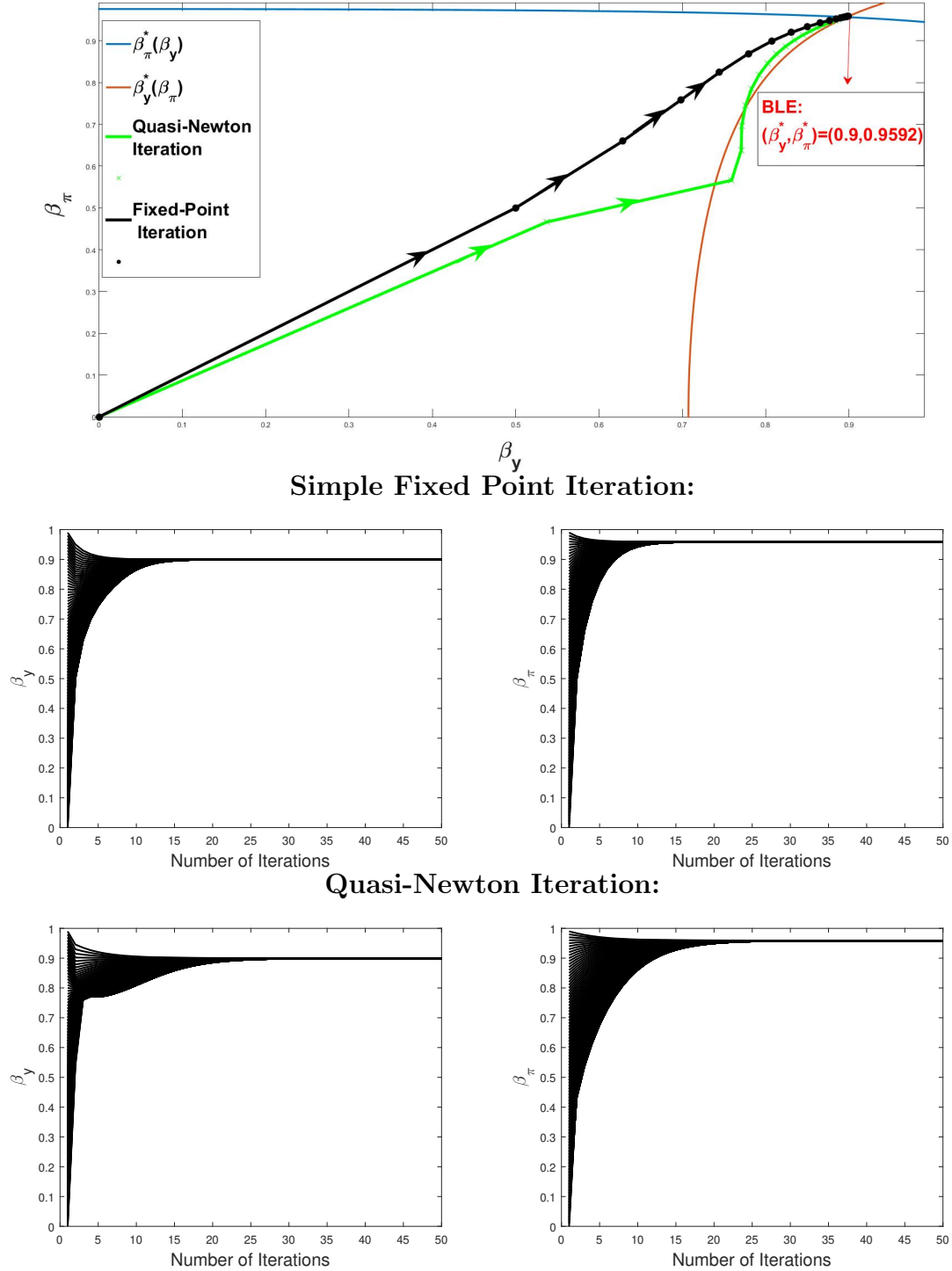
## Multiple BLE

In general, it is not easy to identify parameter regions where multiple E-stable BLE co-exist. Therefore we demonstrate the case of multiple equilibria using the example in Hommes & Zhu (2014), which abstracts away from monetary policy and assumes that output gap $y_t$ follows an exogenous AR(1) process:

$$
\begin{cases}
\pi_t = \lambda \pi_{t+1}^e + \gamma y_t + u_t \\
y_t = a + \rho y_{t-1} + \epsilon_t
\end{cases}
\tag{1.1}
$$

where $u_t$ and $\epsilon_t$ denote white noise processes with variances $\sigma_u$ and $\sigma_\epsilon$ respectively. In this setup, inflation $\pi_t$ is the only forward-looking variable and there are only two learning parameters. Hommes & Zhu (2014) show that, under empirically plausible parameter values, the system features multiple equilibria, namely with $\lambda = 0.99, \gamma = 0.075, a = 0.0004, \rho = 0.9, \sigma_\epsilon = 0.01, \sigma_u = 0.003162$. While the mean parameter is unique at $\alpha_\pi^* = 0.03$, there are three equilibria with respect to the persistence parameter $\beta_\pi$: two stable equilibria at $(\beta_1^*, \beta_3^*) = (0.3066, 0.9961)$ and one unstable equilibrium at $\beta_2^* = 0.7417$ [1], which are illustrated in the top panel of Figure 2. The middle panel of the same figure shows convergence of the fixed point and Quasi-Newton iterations with randomized initial values. In this case, depending on the initial state $\beta_\pi^{(0)}$ the iterations converge to different equilibria. Unlike the previous example, the Quasi-Newton iteration converges faster than the fixed point iteration in general. However, an interesting result that immediately stands out is that, the Quasi-Newton iteration occasionally converges to the unstable equilibrium for initial values close to $\beta_2^*$, while the fixed point iteration always converges to one of the stable equilibria. This confirms the results in Appendix D of Hommes et. al. (2019). Notice that, for values close to $\beta_2^*$, the simple fixed point iteration is not a contraction since $DG_\beta(\beta_\pi) > 1$. In these cases, the iteration is driven upwards or downwards depending on the initial value, until it reaches the basin of attraction for one of the stable BLE and becomes a locally contracting again. This also explains why its convergence is slower in this case compared to the Quasi-Newton iteration, especially for starting values close to $\beta_2^*$. Convergence to unstable equilibria is an undesirable feature of the Quasi-Newton iteration in our context, since these equilibria are not relevant from an empirical point
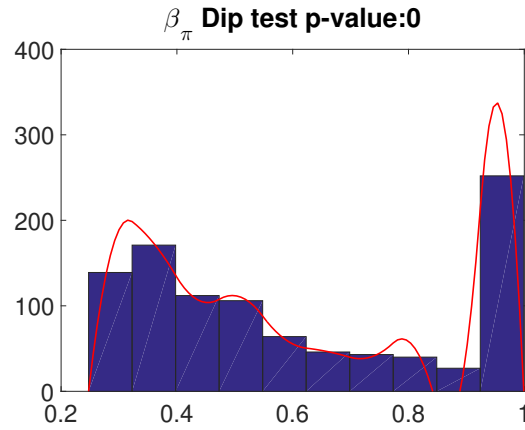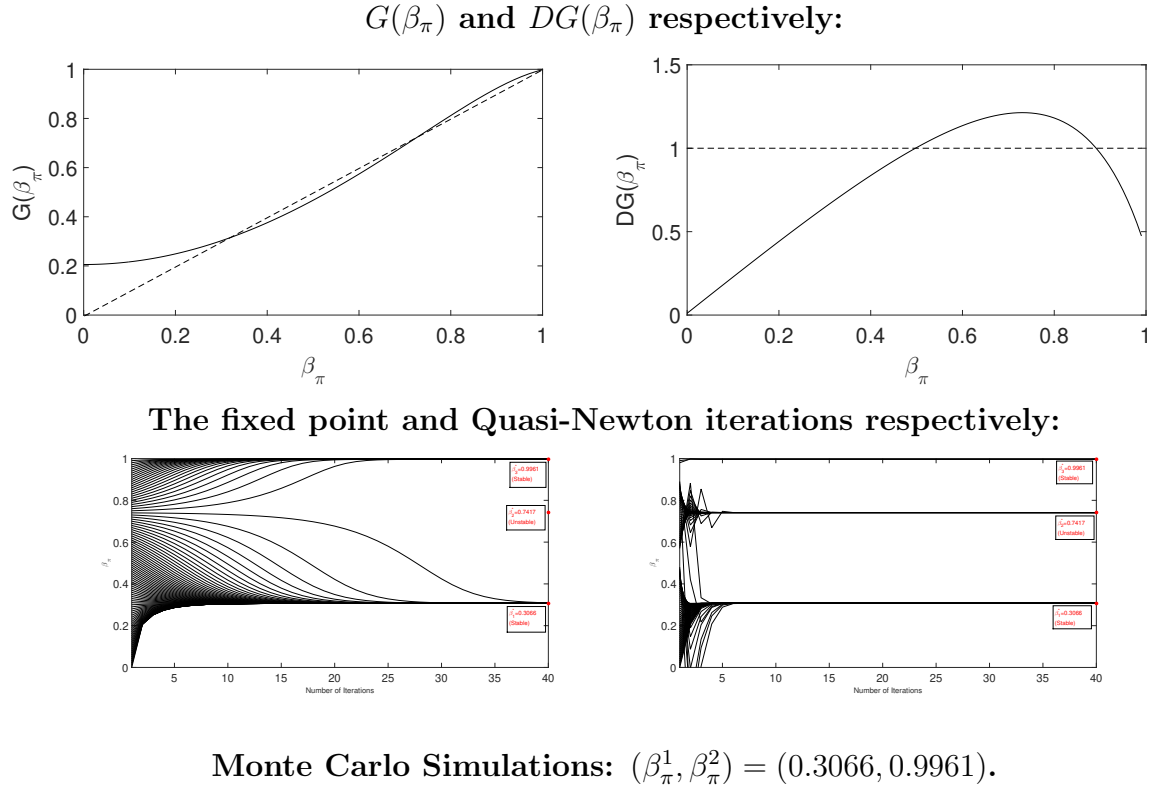
---

[1]Since there is only one forward-looking variable in this case, the mapping $G(.)$ can be analytically computed and is given by $G(\beta_\pi) = \delta \beta_\pi^2 + \dfrac{\gamma^2 \rho (1 - \delta^2 \beta_\pi^4)}{\gamma^2 (\delta \beta_\pi^2 \rho + 1) + (1 - \rho^2)(1 - \delta \beta_\pi^2 \rho) \frac{\sigma_u^2}{\sigma_\epsilon^2}}$.

of view[2]. Figure 2 shows the corresponding histogram resulting from 1000 Monte Carlo simulations of the system with randomized shocks and initial values: it is readily seen that the resulting histogram of $\beta_\pi$ resembles a bimodal distribution with two peaks in the neighbourhoods of the two stable equilibria. The Dip test of unimodality (Hartigan & Hartigan, 1985) result confirms the presence of multiple equilibria, where unimodality is rejected with a p-value of 0.001.

Our results indicate that, in the presence of multiple equilibria, we are able to correctly identify the multiplicity with both iterations, as well as with the Monte Carlo simulations of the system. This is an important point since in general, the expressions for $\boldsymbol{\beta}^* = G(\boldsymbol{\beta}^*)$ are complex enough that we do not know a priori whether the equilibrium at a given parameter set is unique or not. In such systems, the distributions resulting from the Monte Carlo simulations along with the iterations with randomized initial values can be used to examine multiplicity of equilibria. It is important to note that, while iterative E-stability is stronger than E-stability in general, our analysis shows that they are equivalent in the two examples considered so far. Furthermore, we observe that the simple fixed point iteration is more suitable to approximate BLE, since its convergence ensures the iterative E-stability of a given equilibrium, while the Quasi-Newton iteration may result in locally unstable equilibria. More importantly, while the Quasi-Newton approach may take a smaller number of steps to converge in case of multiple equilibria, this approach takes longer in general since the approximation of the Jacobian matrix is a computationally heavy step. Therefore in our paper, we use iterative E-stability as our equilibrium selection criterion and carry out our analysis with the simple fixed point iteration for the empirical validation of BLE.

---

[2]The Quasi-Newton iteration also occasionally leaves the unit circle along the convergence path, which we omit in our figure.

Figure 2: Top panel: The mappings $G(\beta_\pi)$ and $DG(\beta_\pi) = \frac{\partial G(\beta_\pi)}{\partial \beta_\pi}$ that illustrate the multiplicity of equilibria. Middle panel: Convergence of the iterations with randomized initial values. We use a total of 100 iterations in both cases. Bottom panel: Histogram of the learning parameter $\beta_\pi$ resulting from 1000 Monte Carlo simulations, along with the Dip Test result.

## $G(\beta_\pi)$ and $DG(\beta_\pi)$ respectively:



## The fixed point and Quasi-Newton iterations respectively:



## Monte Carlo Simulations: $(\beta_\pi^1, \beta_\pi^2) = (0.3066, 0.9961)$.

# Persistence Amplification

This section provides supplementary results on the persistence amplification of BLE. To illustrate the persistence amplification more clearly, Figure 4 shows the autocorrelation functions of output gap and inflation at the BLE and the REE. Compared with REE, both the autocorrelation functions (ACF) of output gap and inflation at the BLE decay considerably slower. The autocorrelation functions of output gap and inflation are similar to empirical data. Along the BLE, the first-order autocorrelation coefficients of output gap is about 0.9, while after about 5 periods its values decay to about 0.5, which is consistent with empirical work, see for example Fuhrer (2006, 2009). Furthermore, the autocorrelation function of inflation with very high persistence is also close to empirical work for inflation data. That is, for plausible parameters the BLE are capable of reproducing a data-consistent degree of inertia.

Finally, Figure 3 shows that the BLE is stable under SAC-learning, with $\beta_1 \to \beta_1^* \approx 0.9$ and $\beta_2 \to \beta_2^* \approx 0.9592$. In fact, based on our calculation, the two eigenvalues of the Jacobian matrix $\boldsymbol{DG_\beta}(\boldsymbol{\beta}^*)$ are $0.5012 \pm 0.7348i$ (the real parts less than 1), which shows the stability of the BLE under SAC-learning based on our theoretical results.
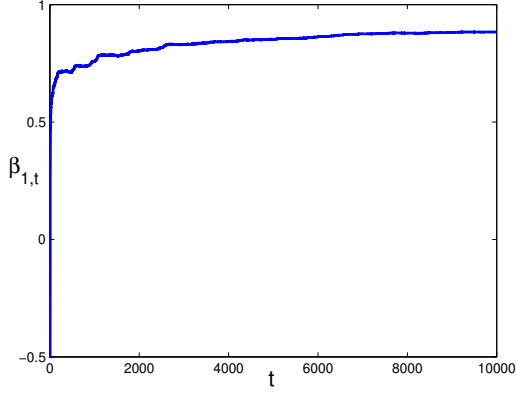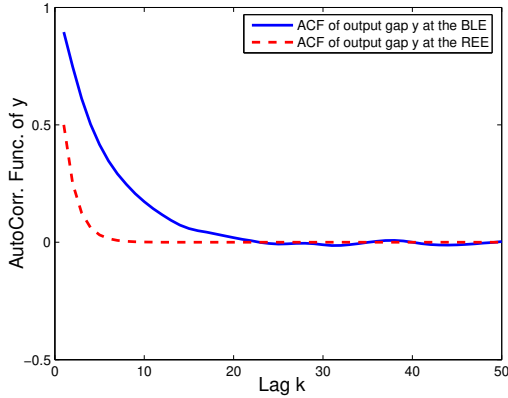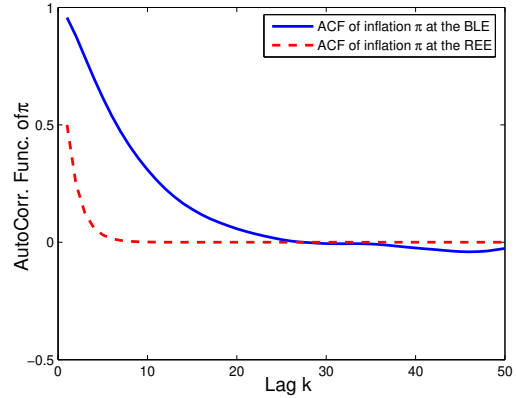
(a) First autocorrelation of $y_t$
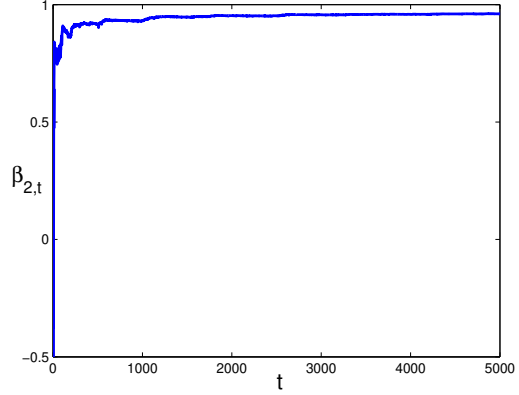


(b) First autocorrelation of $\pi_t$

Figure 3: Time series of $\beta_{1,t}$ and $\beta_{2,t}$ under SAC-learning converging to the BLE $(\beta_1^*, \beta_2^*) = (0.9, 0.9592)$. Parameters are: $\lambda = 0.99, \varphi = 1, \gamma = 0.04, \rho = 0.5, \phi_\pi = 1.5, \phi_y = 0.5, \frac{\sigma_\pi}{\sigma_y} = 0.5$.



(a)



(b)

Figure 4: Autocorrelation functions of output gap $y$ (left) and inflation $\pi$ (right) for contemporaneous Taylor rule at the BLE $(\beta_1^*, \beta_2^*) = (0.9, 0.9592)$ (blue plot) and at the REE $(\beta_1^*, \beta_2^*) = (0.5, 0.5)$ (red plot, dotted line). Parameters are: $\lambda = 0.99, \varphi = 1, \gamma = 0.04, \rho = 0.5, \phi_\pi = 1.5, \phi_y = 0.5, \frac{\sigma_\pi}{\sigma_y} = 0.5$.

# 2 Alternative Taylor Rules

In Hommes et. al. (2019), we consider a contemporaneous Taylor rule throughout the paper. This section provides two altenative Taylor rule specifications with forward- and backward-looking features: we consider the existence and stability conditions, and re-do our optimal monetary policy analysis with our benchmark calibration of structural parameters. Unlike in our paper, we do not consider the variance of interest rate in our loss function in monetary policy analysis.

## 2.1 A forward-looking monetary policy rule

As shown in Bullard and Mitra (2002) and Bullard et al. (2008), an alternative Taylor-type interest rate rule is to assume that the monetary authorities set their interest rate instrument in response to the forecasts of output and inflation deviations. This leads to the forward expectations specification for the interest rate equation with

$$i_t = \phi_\pi \hat{E}_t \pi_{t+1} + \phi_y \hat{E}_t y_{t+1}. \tag{2.1}$$

Thus the New-Keynesian model takes the form of

$$\begin{cases} \mathbf{x}_t = \mathbf{B}\hat{E}_t\mathbf{x}_{t+1} + \mathbf{C}\mathbf{u_t}, \\ \mathbf{u_t} = \boldsymbol{\rho}\mathbf{u_{t-1}} + \boldsymbol{\varepsilon_t}, \end{cases} \tag{2.2}$$

where $\mathbf{B} = \begin{bmatrix} 1 - \varphi\phi_y & \varphi(1-\phi_\pi) \\ \gamma(1-\varphi\phi_y) & \gamma\varphi(1-\phi_\pi) + \lambda \end{bmatrix}$, $\mathbf{C} = \begin{bmatrix} 1 & 0 \\ \gamma & 1 \end{bmatrix}$.

Similar to the above contemporaneous data interest rate rules, if the actual law of motion is stationary, the first-order autocorrelations for inflation and output gap become[3]

$$G_1(\beta_1, \beta_2) = \frac{\widetilde{f}_1}{\widetilde{g}_1} \tag{2.3}$$

$$G_2(\beta_1, \beta_2) = \frac{\widetilde{f}_2}{\widetilde{g}_2} \tag{2.4}$$

---

[3]As in the baseline model above, the first -order sample autocorrelations of output gap and inflation computed based on time series simulations are consistent with the complicated expression for $G_1$ and $G_2$ in Eqs. (2.3-2.4).

where

$$
\begin{aligned}
\widetilde{f}_1 &= \sigma_1^2\Big\{(\rho + \lambda_1 + \lambda_2 - \lambda\beta_2^2)[1 - \lambda\beta_2^2(\rho + \lambda_1 + \lambda_2)] + [\lambda\beta_2^2(\rho\lambda_1 + \rho\lambda_2 + \lambda_1\lambda_2) - \\
&\quad \rho\lambda_1\lambda_2][(\rho\lambda_1 + \rho\lambda_2 + \lambda_1\lambda_2) - \lambda\beta_2^2\rho\lambda_1\lambda_2]\Big\} + \sigma_2^2\Big\{(\varphi(1-\phi_\pi)\beta_2^2)^2[(\rho + \lambda_1 + \lambda_2) \\
&\quad -\rho\lambda_1\lambda_2(\rho\lambda_1 + \rho\lambda_2 + \lambda_1\lambda_2)]\Big\}, \\
\widetilde{g}_1 &= \sigma_1^2\Big\{[(1 + \lambda^2\beta_2^4) - 2\lambda\beta_2^2(\rho + \lambda_1 + \lambda_2) + (1 + \lambda^2\beta_2^4)(\rho\lambda_1 + \rho\lambda_2 + \lambda_1\lambda_2)] \\
&\quad -\rho\lambda_1\lambda_2[(1 + \lambda^2\beta_2^4)(\rho + \lambda_1 + \lambda_2) - 2\lambda\beta_2^2(\rho\lambda_1 + \rho\lambda_2 + \lambda_1\lambda_2) + (1 + \lambda^2\beta_2^4)\rho\lambda_1\lambda_2]\Big\} \\
&\quad +\sigma_2^2\Big\{(\varphi(1-\phi_\pi)\beta_2^2)^2[1 + \rho\lambda_1 + \rho\lambda_2 + \lambda_1\lambda_2 - \rho\lambda_1\lambda_2(\rho + \lambda_1 + \lambda_2) - (\rho\lambda_1\lambda_2)^2]\Big\},
\end{aligned}
$$

$$
\begin{aligned}
\widetilde{f}_2 &= \sigma_1^2\Big\{\gamma^2[(\rho + \lambda_1 + \lambda_2) - \rho\lambda_1\lambda_2(\rho\lambda_1 + \rho\lambda_2 + \lambda_1\lambda_2)]\Big\} + \sigma_2^2\Big\{[(\rho + \lambda_1 + \lambda_2) - (1 - \varphi\phi_y)\beta_1^2]\cdot \\
&\quad [1 - (1 - \varphi\phi_y)\beta_1^2(\rho + \lambda_1 + \lambda_2)] + [(1 - \varphi\phi_y)\beta_1^2(\rho\lambda_1 + \rho\lambda_2 + \lambda_1\lambda_2) - \rho\lambda_1\lambda_2]\cdot \\
&\quad [(\rho\lambda_1 + \rho\lambda_2 + \lambda_1\lambda_2) - (1 - \varphi\phi_y)\beta_1^2\rho\lambda_1\lambda_2]\Big\}, \\
\widetilde{g}_2 &= \sigma_1^2\Big\{\gamma^2[1 + \rho\lambda_1 + \rho\lambda_2 + \lambda_1\lambda_2 - \rho\lambda_1\lambda_2(\rho + \lambda_1 + \lambda_2) - (\rho\lambda_1\lambda_2)^2]\Big\} \\
&\quad +\sigma_2^2\Big\{[1 + ((1 - \varphi\phi_y)\beta_1^2)^2 - 2(1 - \varphi\phi_y)\beta_1^2(\rho + \lambda_1 + \lambda_2) + (1 + ((1 - \varphi\phi_y)\beta_1^2)^2)\cdot \\
&\quad (\rho\lambda_1 + \rho\lambda_2 + \lambda_1\lambda_2)] - \rho\lambda_1\lambda_2[(1 + ((1 - \varphi\phi_y)\beta_1^2)^2)(\rho + \lambda_1 + \lambda_2) - 2(1 - \varphi\phi_y)\beta_1^2\cdot \\
&\quad (\rho\lambda_1 + \rho\lambda_2 + \lambda_1\lambda_2) + (1 + ((1 - \varphi\phi_y)\beta_1^2)^2)\rho\lambda_1\lambda_2]\Big\},
\end{aligned}
$$

$$
\begin{aligned}
\lambda_1 + \lambda_2 &= (1 - \varphi\phi_y)\beta_1^2 + (\gamma\varphi(1-\phi_\pi) + \lambda)\beta_2^2, \\
\lambda_1\lambda_2 &= \lambda(1 - \varphi\phi_y)\beta_1^2\beta_2^2.
\end{aligned}
$$

In this case we have some similar results on the existence and stability as in the baseline model. Since the coefficients matrices are different, the corresponding sufficient conditions change.

**Corollary 1** *Under the forward-looking interest rate rule, if $\phi_y < \frac{1}{\varphi}$ and $1 < \phi_\pi < 1 + \frac{\lambda}{\gamma\varphi}$, then there exists at least one BLE $(\boldsymbol{\alpha}^*, \boldsymbol{\beta}^*)$, where $\boldsymbol{\alpha}^* = \mathbf{0} = \overline{\mathbf{x}}^*$. Furthermore, the BLE $(\boldsymbol{\alpha}^*, \boldsymbol{\beta}^*)$ is locally stable under SAC-learning if all the eigenvalues of $\boldsymbol{DG_\beta}(\boldsymbol{\beta}^*) = \left(\frac{\partial G_i}{\partial \beta_j}\right)_{\boldsymbol{\beta}=\boldsymbol{\beta}^*}$ have real parts less than 1.*

**Proof.** See Appendix A.

For the same benchmark parameter values as in the contemporaneous Taylor rule, the system has a BLE $(\beta_1^*, \beta_2^*) = (0.8326, 0.9605)$, with output and inflation much more persistent than the REE benchmark (with $\rho = 0.5$), as illustrated in Figure 5. Figure 6a
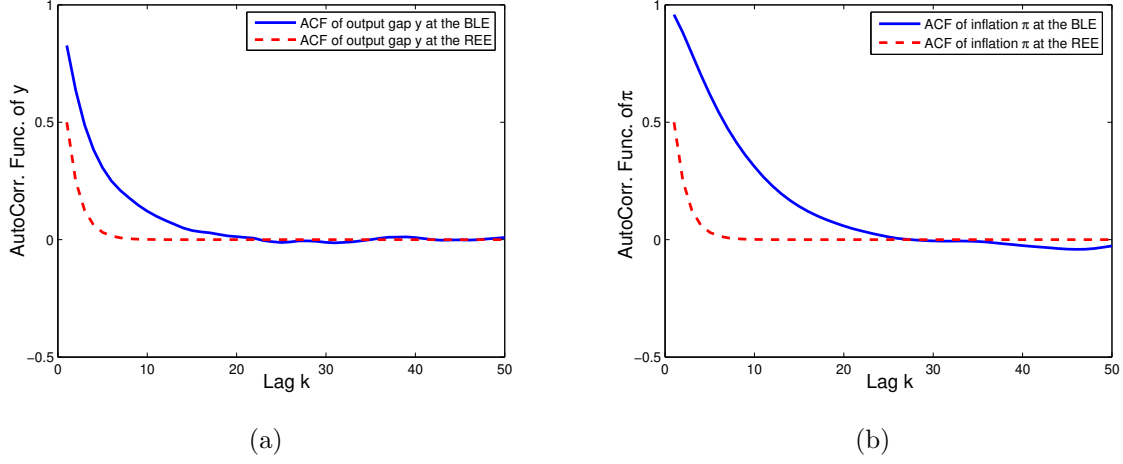
10

Figure 5: Autocorrelation functions of output gap $y$ and inflation $\pi$ with forward-looking Taylor rule at the BLE $(\beta_1^*, \beta_2^*) = (0.8326, 0.9605)$. Parameters are: $\lambda = 0.99, \varphi = 1, \gamma = 0.04, \rho = 0.5, \phi_\pi = 1.5, \phi_y = 0.5, \sigma_2/\sigma_1 = 0.5$.
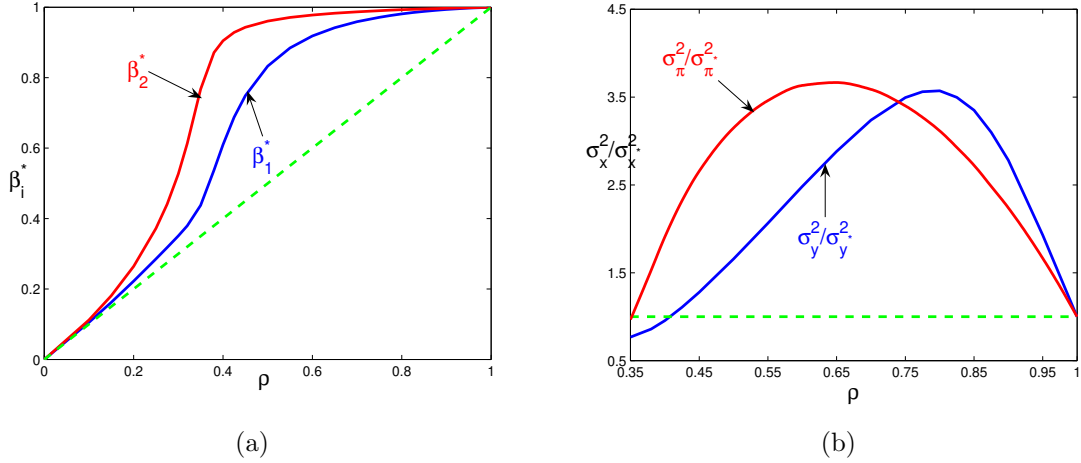


Figure 6: BLE $(\beta_1^*, \beta_2^*)$ as a function of the persistence $\rho$ of the exogenous shocks with forward-looking Taylor rule (a) $\beta_i^*(i = 1, 2)$ with respect to $\rho$; (b) the ratio of variances $(\sigma_y^2/\sigma_{y^*}^2, \sigma_\pi^2/\sigma_{\pi^*}^2)$ with respect to $\rho$ at the corresponding BLE $(\beta_1^*, \beta_2^*)$. Parameters are: $\lambda = 0.99, \varphi = 1, \gamma = 0.04, \phi_\pi = 1.5, \phi_y = 0.5, \frac{\sigma_\pi}{\sigma_y} = 0.5$.

illustrates how these results depend on the parameter $\rho$, the persistence of the exogenous shocks. As before, for the forward looking Taylor rule, the system also displays *persistence amplification*, with the persistence of inflation and output gap along BLE much higher than the persistence $\rho$ of the exogenous shocks. Similarly, Figure 6b illustrates the excess volatility of inflation and output compared to the REE benchmark.

Here we also find finite optimal coefficients as for the contemporaneous Taylor rule. The difference is that here the optimal policy is $(\phi_y^*, \phi_\pi^*) = (1.1793, 10.7942)$, which are both higher than in the contemporaneous case. We further study how the finite optimal coefficients respond as the persistence $\rho$ of shocks and the weight $\omega$ on inflation change. Figure 7a indicates that the finite optimal $\phi_\pi^*$ increases as $\rho$ varies around 0.5, while $\phi_y^*$ changes only a little. This is because in this case the ratio $\sigma_\pi^2/\sigma_y^2$ of variances of inflation and output gap is relatively larger than in the contemporaneous case. For example, given the benchmark parameters, the variances of output gap and inflation at the BLE are 3.963 and 4.097 while they are 3.855 and 3.595, respectively, in the contemporaneous case. So here the variance of inflation plays a more important role and the finite optimal policy $\phi_\pi^*$ changes faster than $\phi_y^*$. Figure 8 suggests similar effects of the weight of inflation $\omega$ on the finite optimal coefficients and optimal manifolds. Similar to the contemporaneous case, the optimal manifold moves up generally as $\rho$ or $\omega$ grows. In addition, Figure 8b suggests that, as before, $\phi_\pi^* \approx 1.5$, if $\phi_y^* = 0.5$ in the optimal manifold for $\omega = 0.5$ in the framework of BLE and the loss function decreases very slowly till the finite optimal policy after $\phi_y^* = 0.5$, as shown in Figure 9.
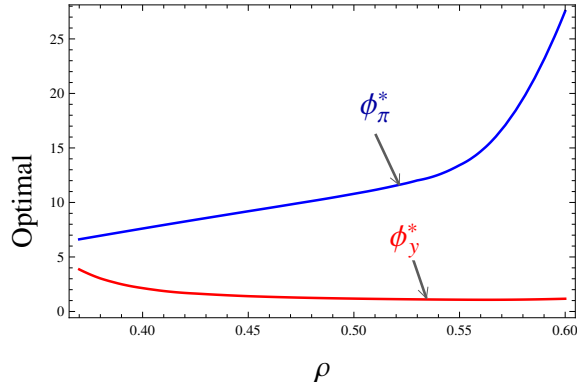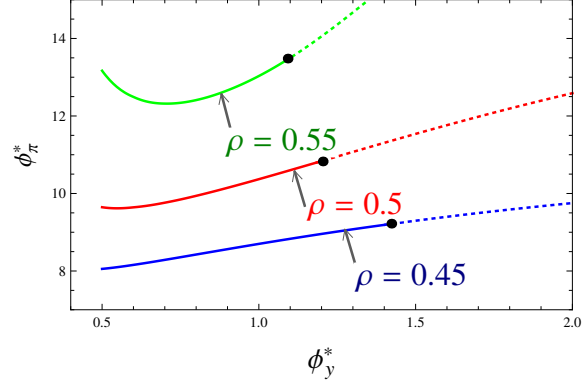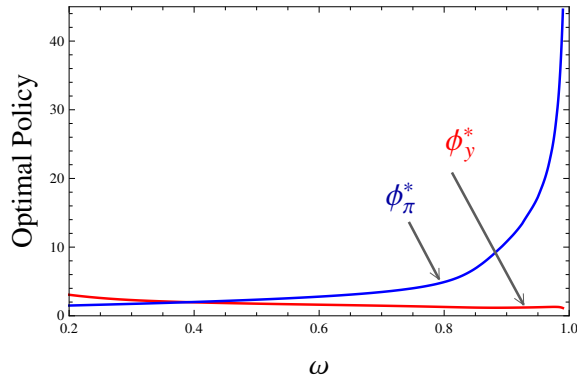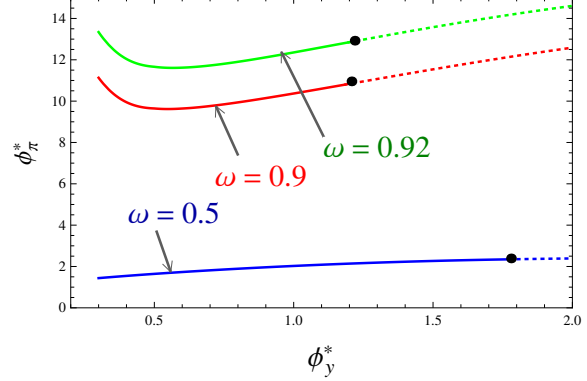
| (a) Optimal policy | (b) Optimal manifold |

Figure 7: Optimal policies at the BLE with respect to $\rho$ (a) and corresponding optimal manifolds for three different $\rho$ (connection points of solid and dotted curves corresponding to finite optimal policies) (b) with the forward-looking interest rate rule. Parameters are: $\lambda = 0.99, \varphi = 1, \gamma = 0.04, \frac{\sigma_\pi}{\sigma_y} = 0.5$ and $\omega = 0.9$.



| (a) Optimal policy | (b) Optimal manifold |

Figure 8: Optimal policies at the BLE with respect to $\omega$ (a) and corresponding optimal manifolds for three different $\omega$ (connection points of solid and dotted curves corresponding to finite optimal policies) (b) with the forward-looking interest rate rule. Parameters are: $\lambda = 0.99, \varphi = 1, \gamma = 0.04, \sigma_\pi/\sigma_y = 0.5$ and $\rho = 0.5$.
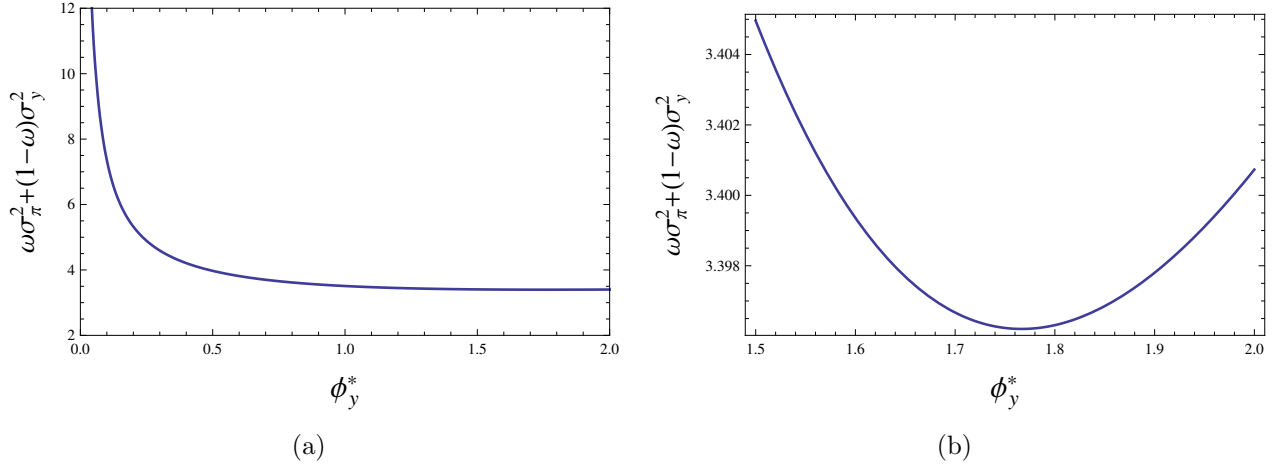
Figure 9: Loss function along the optimal manifold in Figure 8(b) with $\omega = 0.5$ for different ranges of $\phi_y^*$, i.e. $\phi_y^* \in [0, 2]$ (a) and $\phi_y^* \in [1.5, 2]$ (b). Parameters are: $\lambda = 0.99, \varphi = 1, \gamma = 0.04, \rho = 0.5, \frac{\sigma_\pi}{\sigma_y} = 0.5$ and $\omega = 0.5$.

## 2.2    A lagged monetary policy rule

As argued e.g. in Bullard and Mitra (2002), it may be viewed as realistic for central bank practice to posit that the monetary authorities must react to last quarter's observations on inflation and output gap as contemporaneous values are not known yet. This leads to the lagged data specification for the interest rate equation, where (??) is replaced by

$$i_t = \phi_\pi \pi_{t-1} + \phi_y y_{t-1}. \tag{2.5}$$

The New-Keynesian model becomes

$$\begin{cases} \boldsymbol{x}_t = \boldsymbol{A}\boldsymbol{x}_{t-1} + \boldsymbol{B}\boldsymbol{x}_{t+1}^e + \boldsymbol{C}\boldsymbol{u}_t, \\ \boldsymbol{u}_t = \boldsymbol{\rho}\boldsymbol{u}_{t-1} + \boldsymbol{\varepsilon}_t, \end{cases} \tag{2.6}$$

where $\boldsymbol{A} = \begin{bmatrix} -\varphi\phi_y & -\varphi\phi_\pi \\ -\gamma\varphi\phi_y & -\gamma\varphi\phi_\pi \end{bmatrix}$, $\boldsymbol{B} = \begin{bmatrix} 1 & \varphi \\ \gamma & \gamma\varphi + \lambda \end{bmatrix}$, $\boldsymbol{C} = \begin{bmatrix} 1 & 0 \\ \gamma & 1 \end{bmatrix}$.

Similar to the contemporaneous and forward-looking Taylor rules, if the actual law of motion is stationary, the first-order autocorrelations for output gap and inflation become

$$G_1(\beta_1, \beta_2) = \frac{\widetilde{f_1}}{\widetilde{g_1}} \tag{2.7}$$

$$G_2(\beta_1, \beta_2) = \frac{\widetilde{f_2}}{\widetilde{g_2}} \tag{2.8}$$

14

where

$$
\begin{aligned}
\widetilde{f_1} &= \sigma_y^2\Big\{(\rho + \lambda_1 + \lambda_2 - \lambda\beta_2^2)[1 - \lambda\beta_2^2(\rho + \lambda_1 + \lambda_2)] + [\lambda\beta_2^2(\rho\lambda_1 + \rho\lambda_2 + \lambda_1\lambda_2) - \\
&\quad \rho\lambda_1\lambda_2][(\rho\lambda_1 + \rho\lambda_2 + \lambda_1\lambda_2) - \lambda\beta_2^2\rho\lambda_1\lambda_2]\Big\} + \sigma_\pi^2\Big\{(\varphi\phi_\pi - \varphi\beta_2^2)^2[(\rho + \lambda_1 + \lambda_2) \\
&\quad -\rho\lambda_1\lambda_2(\rho\lambda_1 + \rho\lambda_2 + \lambda_1\lambda_2)]\Big\}, \\
\widetilde{g_1} &= \sigma_y^2\Big\{[(1 + \lambda^2\beta_2^4) - 2\lambda\beta_2^2(\rho + \lambda_1 + \lambda_2) + (1 + \lambda^2\beta_2^4)(\rho\lambda_1 + \rho\lambda_2 + \lambda_1\lambda_2)] \\
&\quad -\rho\lambda_1\lambda_2[(1 + \lambda^2\beta_2^4)(\rho + \lambda_1 + \lambda_2) - 2\lambda\beta_2^2(\rho\lambda_1 + \rho\lambda_2 + \lambda_1\lambda_2) + (1 + \lambda^2\beta_2^4)\rho\lambda_1\lambda_2]\Big\} \\
&\quad +\sigma_\pi^2\Big\{(\varphi\phi_\pi - \varphi\beta_2^2)^2[1 + \rho\lambda_1 + \rho\lambda_2 + \lambda_1\lambda_2 - \rho\lambda_1\lambda_2(\rho + \lambda_1 + \lambda_2) - (\rho\lambda_1\lambda_2)^2]\Big\},
\end{aligned}
$$

$$
\begin{aligned}
\widetilde{f_2} &= \sigma_y^2\Big\{\gamma^2[(\rho + \lambda_1 + \lambda_2) - \rho\lambda_1\lambda_2(\rho\lambda_1 + \rho\lambda_2 + \lambda_1\lambda_2)]\Big\} + \sigma_\pi^2\Big\{[(\rho + \lambda_1 + \lambda_2) - (\beta_1^2 - \varphi\phi_y)] \cdot \\
&\quad [1 - (\beta_1^2 - \varphi\phi_y)(\rho + \lambda_1 + \lambda_2)] + [(\beta_1^2 - \varphi\phi_y)(\rho\lambda_1 + \rho\lambda_2 + \lambda_1\lambda_2) - \rho\lambda_1\lambda_2] \cdot \\
&\quad [(\rho\lambda_1 + \rho\lambda_2 + \lambda_1\lambda_2) - (\beta_1^2 - \varphi\phi_y)\rho\lambda_1\lambda_2]\Big\}, \\
\widetilde{g_2} &= \sigma_y^2\Big\{\gamma^2[1 + \rho\lambda_1 + \rho\lambda_2 + \lambda_1\lambda_2 - \rho\lambda_1\lambda_2(\rho + \lambda_1 + \lambda_2) - (\rho\lambda_1\lambda_2)^2]\Big\} \\
&\quad +\sigma_\pi^2\Big\{[(1 + (\beta_1^2 - \varphi\phi_y)^2) - 2(\beta_1^2 - \varphi\phi_y)(\rho + \lambda_1 + \lambda_2) + (1 + (\beta_1^2 - \varphi\phi_y)^2) \cdot \\
&\quad (\rho\lambda_1 + \rho\lambda_2 + \lambda_1\lambda_2)] - \rho\lambda_1\lambda_2[(1 + (\beta_1^2 - \varphi\phi_y)^2)(\rho + \lambda_1 + \lambda_2) - 2(\beta_1^2 - \varphi\phi_y) \cdot \\
&\quad (\rho\lambda_1 + \rho\lambda_2 + \lambda_1\lambda_2) + (1 + (\beta_1^2 - \varphi\phi_y)^2)\rho\lambda_1\lambda_2]\Big\},
\end{aligned}
$$

$$
\begin{aligned}
\lambda_1 + \lambda_2 &= \beta_1^2 - \varphi\phi_y - \gamma\varphi\phi_\pi + (\gamma\varphi + \lambda)\beta_2^2, \\
\lambda_1\lambda_2 &= \lambda(\beta_1^2 - \varphi\phi_y)\beta_2^2.
\end{aligned}
$$

Note that, because of the additional lagged term $x_{t-1}$, the rational expectations equilibrium is different compared to the system without this lagged term $\boldsymbol{x}_{t-1}$ in the previous two cases. In this case we have similar results on the existence and stability on BLE as in the baseline model.

**Corollary 2** *Under the lagged interest rate rule, if $\phi_y < \frac{1}{\varphi}$ and $1 < \phi_\pi < \frac{1 - \varphi\phi_y}{\gamma\varphi}$, then there exists at least one BLE $(\boldsymbol{\alpha}^*, \boldsymbol{\beta}^*)$. Furthermore, the BLE $(\boldsymbol{\alpha}^*, \boldsymbol{\beta}^*)$ is locally stable under SAC-learning if all the eigenvalues of $\boldsymbol{DG_\beta}(\boldsymbol{\beta}^*) = \left(\frac{\partial G_i}{\partial \beta_j}\right)_{\boldsymbol{\beta} = \boldsymbol{\beta}^*}$ have real parts less than 1.*

**Proof.** See Appendix B.

For the same benchmark parameter values as before, the system has a BLE $(\beta_1^*, \beta_2^*) = (0.7746, 0.9628)$. Figure 10 illustrates the ACF of output and inflation along the BLE
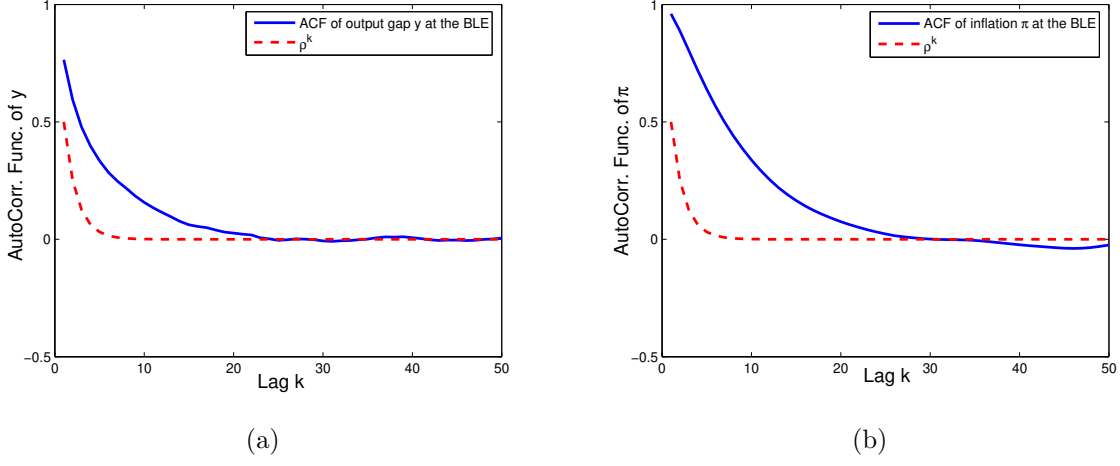
(a)

(b)

Figure 10: Autocorrelation functions of output gap $y$ and inflation $\pi$ with lagged Taylor rule at the BLE $(\beta_1^*, \beta_2^*) = (0.7746, 0.9628)$. Parameters are: $\lambda = 0.99, \varphi = 1, \gamma = 0.04, \rho = 0.5, \phi_\pi = 1.5, \phi_y = 0.5, \sigma_y/\sigma_\pi = 0.5$.
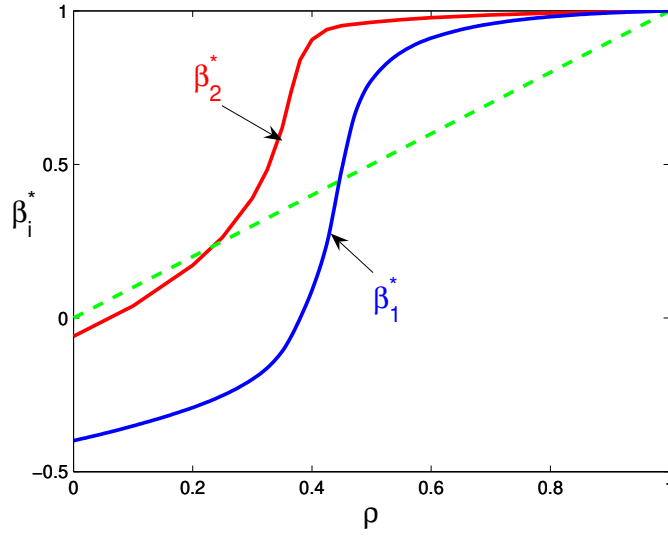


Figure 11: Effects of $\rho$ with lagged Taylor rule, i.e. $\beta_i^*(i = 1, 2)$ with respect to $\rho$. Parameters are: $\lambda = 0.99, \varphi = 1, \gamma = 0.04, \phi_\pi = 1.5, \phi_y = 0.5, \frac{\sigma_y}{\sigma_\pi} = 0.5$.
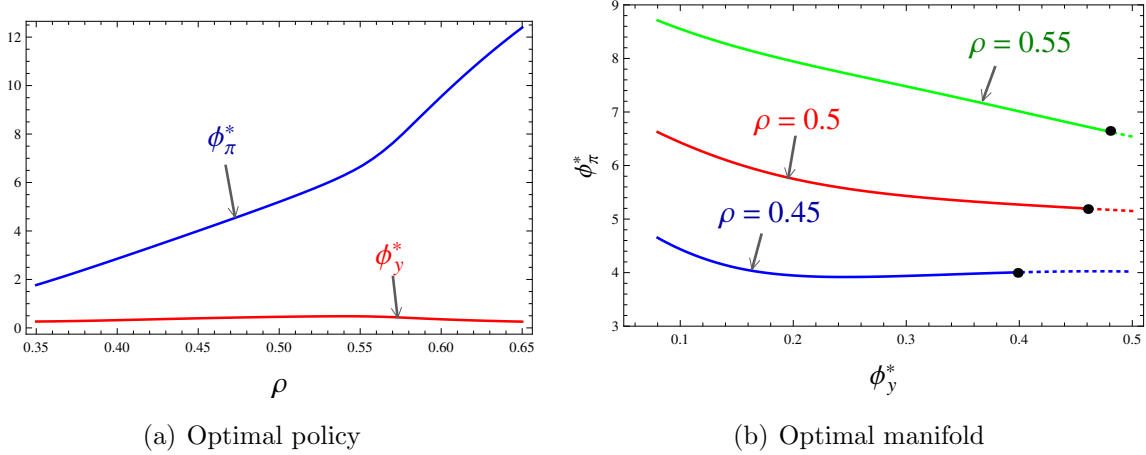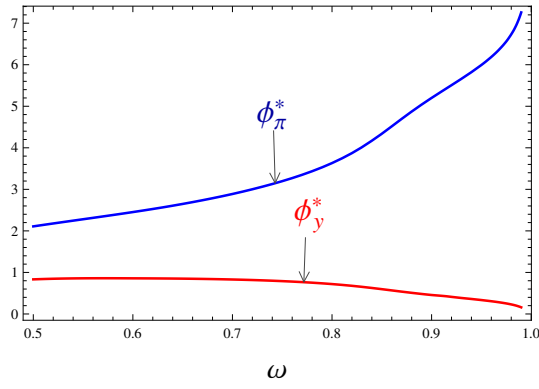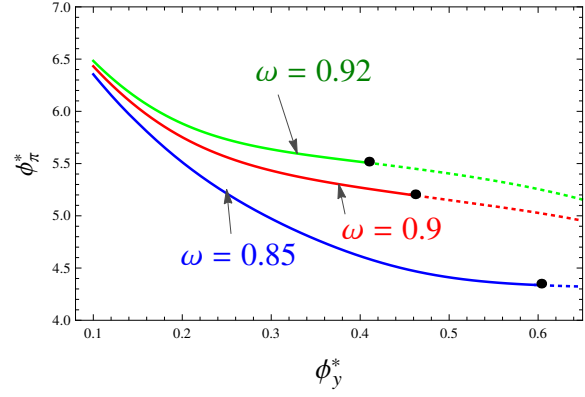
(a) Optimal policy                    (b) Optimal manifold

Figure 12: Optimal policies at the BLE with respect to $\rho$ (a) and corresponding optimal manifolds for three different $\rho$ (connection points of solid and dotted curves corresponding to finite optimal policies) (b) with the lagged interest rate rule. Parameters are: $\lambda = 0.99, \varphi = 1, \gamma = 0.04, \sigma_\pi/\sigma_y = 0.5$ and $\omega = 0.9$.

and shows that they are much more persistent than the autocorrelations in the exogenous shocks. Figure 11 illustrates that the model with a lagged Taylor rule also exhibits *persistence amplification* within the empirically relevant region of parameters $\rho \geq 0.5$.

Here we find finite optimal coefficients again as in the contemporaneous and forward-looking Taylor rules. The difference is that here the optimal policy is $(\phi_y^*, \phi_\pi^*) = (0.4566, 5.2008)$. We further study how the finite optimal coefficients respond as the persistence $\rho$ of shocks and the weight on inflation $\omega$ change. Figure 12a indicates that finite optimal $\phi_\pi^*$ increases as $\rho$ varies around 0.5 while $\phi_y^*$ changes just a little, similar to the forward-looking case. This is also because in this case the ratio of variances of inflation and output gap is also larger than in the contemporaneous case, that is, the variance of inflation plays a more dominant role. For example, given the benchmark parameters, the variances of output gap and inflation at the BLE are 3.145 and 4.310, while they are 3.855 and 3.595, respectively, in the contemporaneous case. Therefore, similar to the forward-looking case, the finite optimal policy $\phi_\pi^*$ changes faster than $\phi_y^*$. Figure 13 suggests similar effects of the weight on inflation $\omega$ on the finite optimal coefficients and optimal manifolds. In addition, if we consider $\omega = 0.5$, Figure 14 suggests that, as before, $(\phi_y^*, \phi_\pi^*) = (0.5, 1.5)$ is nearly optimal in the case the weight $\omega = 0.5$.

17

(a) Optimal policy  (b) Optimal manifold

Figure 13: Optimal policies at the BLE with respect to $\omega$ (a) and corresponding optimal manifolds for three different $\omega$ (connection points of solid and dotted curves corresponding to finite optimal policies) (b) with the lagged interest rate rule. Parameters are: $\lambda = 0.99, \varphi = 1, \gamma = 0.04, \sigma_\pi/\sigma_y = 0.5$ and $\rho = 0.5$.
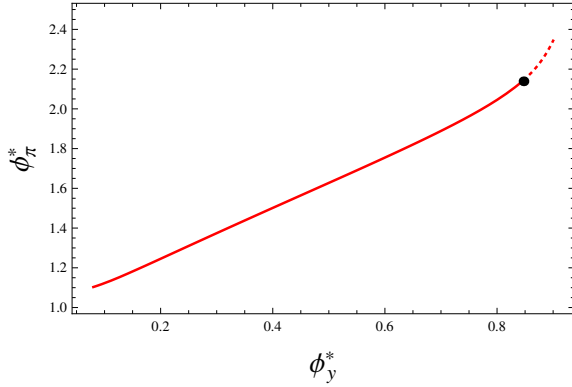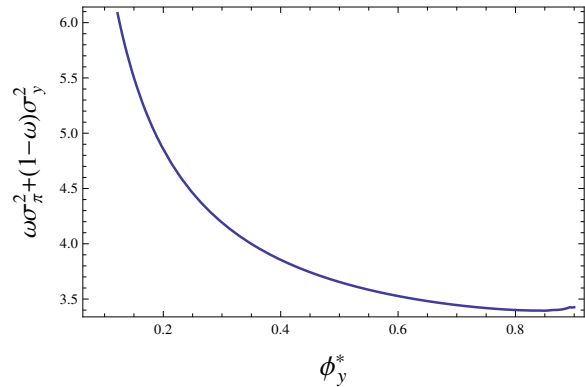


(a) Optimal manifold  (b) Loss function

Figure 14: Optimal manifold at the BLE for $\omega = 0.5$ (connection points of solid and dotted curves corresponding to finite optimal policies) (a) and corresponding loss function along the optimal manifold(b) with the lagged interest rate rule. Parameters are: $\lambda = 0.99, \varphi = 1, \gamma = 0.04, \rho = 0.5, \sigma_\pi/\sigma_y = 0.5, \omega = 0.5$.

## 2.3　Alternative Model Specifications

This section provides supplementary material for our empirical results under BLE. As an alternative to the benchmark New-Keynesian model, we consider a hybrid version of the model with lagged inflation and output gap:

$$
\begin{cases}
y_t = (1 - \iota_y)y_{t+1}^e + \iota_y y_{t-1} - \varphi(i_t - \pi_{t+1}^e) + u_{y,t}, \\
\pi_t = \lambda((1 - \iota_p)\pi_{t+1}^e + \iota_p \pi_{t-1}) + \gamma y_t + u_{\pi,t},
\end{cases}
\tag{2.9}
$$

We further provide estimation results under the alternative monetary policy rules considered in the previous section. Table 1 shows the estimation results obtained from our estimation algorithm in Hommes et. al. (2019). To briefly discuss the results in Table 1, consider first the specification with the backward-looking inflation and output gap. In this case some of the exogenous persistence shifts towards the backward-looking parameters $\iota_p$ and $\iota_y$ under both BLE and RE. In particular, notice that $\rho_\pi$ decreases to near-zero levels under both models, and the persistence is generated almost exclusively through $\iota_p$. This parameter is slightly higher under RE as one might expect, which suggests that persistence amplification under BLE is still larger. For output gap, we observe similar estimated values for $\iota_y$ under both BLE and RE, while $\rho_y$ is substantially smaller under BLE. This is similar to our baseline specification without the backward-looking terms. This exercise shows that, with the addition of the backward-looking terms, the REE essentially becomes a mix of the purely forward-looking REE, and the purely backward-looking BLE. Hence there is some persistence amplification under REE in this case, but less than BLE. The Laplace estimators suggest that the model fit under BLE is still substantially better compared with REE. Next consider the results under the backward-looking Taylor rule. This specification results in little to no change in parameter estimates under both specifications, but the likelihood deteriorates under both cases compared to the contemporenous Taylor rule, suggesting that this rule is not favored by the data. Similar results also emerge under the forward-looking Taylor rule for BLE: the parameter estimates and the Laplace approximation are very similar to the backward-looking rule. This result is expected since both rules have very similar functional forms under BLE. For RE, the results are slightly different under the forward-looking rule and the likelihood improves quite a bit. In particular, under the forward-looking rule without lagged inflation and output gap, RE yields a better likelihood compared to BLE. It is important to note that this result arises mostly due to the worsening likelihood under BLE with forward-

looking rule, rather than a substantial improvement in likelihood under REE. Overall, the parameter estimates under our baseline estimations with contemporaneous Taylor rule seems robust to these alternative specifications.

| | BLE | REE | BLE, Backward MP | REE, Backward MP | BLE,Forward MP | | REE Forward MP | |
|---|---|---|---|---|---|---|---|---|
| | -326.13 | -350.06 | -353.3 | -370.32 | -352.73 | -341.25 | -348.06 | -344.1 |
| $\sigma_y$ | 0.73 | 0.15 | 0.72 | 0.12 | 0.72 | 0.74 | 0.15 | 0.16 |
| $\sigma_\pi$ | 0.27 | 0.15 | 0.3 | 0.04 | 0.29 | 0.27 | 0.04 | 0.15 |
| $\sigma_r$ | 0.29 | 0.3 | 0.3 | 0.31 | 0.3 | 0.3 | 0.3 | 0.3 |
| $\bar{y}$ | -0.13 | -0.18 | -0.11 | -0.18 | -0.13 | -0.2 | -0.18 | -0.18 |
| $\bar{\pi}$ | 0.64 | 0.66 | 0.8 | 0.69 | 0.8 | 0.56 | 0.7 | 0.67 |
| $\bar{r}$ | 0.95 | 0.92 | 1.11 | 1.01 | 1.13 | 0.89 | 0.99 | 0.95 |
| $\gamma$ | 0.03 | 0.01 | 0.02 | 0.01 | 0.02 | 0.02 | 0.01 | 0.01 |
| $\frac{1}{\varphi}$ | 3.29 | 4.53 | 3.63 | 5.08 | 3.62 | 3.56 | 4.28 | 4.29 |
| $\phi_\pi$ | 1.35 | 1.42 | 1.33 | 1.29 | 1.56 | 1.37 | 1.54 | 1.63 |
| $\phi_y$ | 0.48 | 0.46 | 0.32 | 0.27 | 0.39 | 0.33 | 0.54 | 0.54 |
| $\rho_\pi$ | 0.03 | 0.03 | 0.32 | 0.87 | 0.31 | 0.02 | 0.87 | 0.03 |
| $\rho_y$ | 0.3 | 0.86 | 0.36 | 0.89 | 0.36 | 0.25 | 0.89 | 0.85 |
| $\rho_r$ | 0.85 | 0.79 | 0.87 | 0.77 | 0.87 | 0.87 | 0.78 | 0.78 |
| $\iota_y$ | 0.24 | 0.21 | - | - | | 0.24 | | 0.28 |
| $\iota_\pi$ | 0.43 | 0.52 | - | - | | 0.31 | | 0.52 |

Table 1: Estimation results with the Hybrid NK model and alternative monetary policy rules

## 2.4 Monetary Policy and Multiplicity of Equilibria

We finish this online appendix with an illustration of how multiplicity of equilibria can arise under BLE when monetary policy parameters are varied. In all calibration and estimation exercises that we discussed so far for the New-Keynesian model, the underlying BLE is unique. However, multiple stable BLE can arise for certain combinations of parameter values. One such case can be observed when we set the parameter values to their CBO-based output gap estimations as given in Hommes et. al. (2019) and vary the values of monetary policy parameters. In this case the estimated Philips curve slope $\gamma$ is smaller at 0.024 compared with our benchmark estimation with $\gamma = 0.035$. Figure **??** illustrates how inflation and output gap variances change as we vary the monetary policy coefficients $\phi_y \in [0.25, 0.5]$ and $\phi_\pi \in [1, 1.75]$ in this case. While the change in variances follow the same overall pattern as in the benchmark case, we observe two co-existing E-stable BLE over a small range of parameter values. The underlying BLE is unique at the estimated parameter values, but as the reaction coefficients become smaller, with $\phi_y < 0.33$ or $\phi_\pi < 1.3$, another BLE with higher variance and higher persistence for both inflation and output gap becomes stable and there is a range of parameter values where these two stable BLE co-exist. For smaller values of reaction coefficients, with $\phi_y < 0.31$ or $\phi_\pi < 1.1$, the low persistence/low variance equilibrium becomes unstable and only the high-variance equilibrium remains. These results suggest that, for certain parameter combinations, there is another important role for monetary policy in terms of ensuring that such high volatility equilibria are destabilized, which is only possible with a sufficiently active policy rule. In our example multiplicity of equilibria is driven by a flatter Philips curve compared to our benchmark case, but similar results can arise when other structural parameters are varied, such as the exogenous shock persistence parameters $\rho_y$ and $\rho_\pi$, or the intertemporal elasticity of substitution $\varphi$.
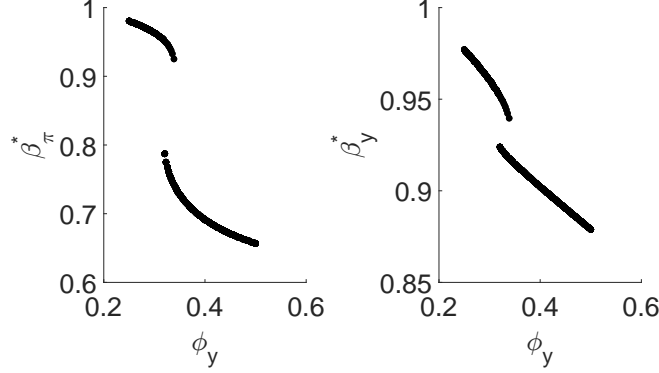
(a) Variances $\sigma_y^2$ and $\sigma_\pi^2$ w.r.t. $\phi_y$

Figure 15: Optimal Policy under BLE and REE at the estimated parameter values.

Figure 16: Multiple iteratively E-stable BLE.

# Appendix

# A    Proof of Corollary 1

Under the forward looking expectations interest rate rule, the characteristic polynomial of $\boldsymbol{B\beta}^2$ is given by $h(\nu) = \nu^2 + c_1\nu + c_2$, where

$$c_1 = -[(1 - \varphi\phi_y)\beta_1^2 + (\gamma\varphi(1 - \phi_\pi) + \lambda)\beta_2^2], \quad c_2 = \lambda(1 - \varphi\phi_y)\beta_1^2\beta_2^2.$$

Similarly, both of the eigenvalues of $\boldsymbol{B\beta}^2$ are inside the unit circle if and only if the following conditions hold (see Elaydi, 1999): $h(1) > 0, \quad h(-1) > 0, \quad |h(0)| < 1$. Based on our assumption $\phi_y < \frac{1}{\varphi}$ and $1 < \phi_\pi < 1 + \frac{\lambda}{\gamma\varphi}$, it is easy to see $c_1 \le 0$ and $0 \le h(0) < 1$, and hence $h(-1) > 0$ for any $\beta_i \in [-1, 1]$. Furthermore

$$h(1) = (1 - \beta_1^2)(1 - \lambda\beta_2^2) + \gamma\varphi(\phi_\pi - 1)\beta_2^2 + \varphi\phi_y\beta_1^2(1 - \lambda\beta_2^2) > 0. \qquad (A.1)$$

In addition, for the stability of BLE, we need to show both eigenvalues of $(\boldsymbol{I} - \boldsymbol{B\beta}^2)^{-1}(\boldsymbol{B} - \boldsymbol{I})$ have negative real parts if $\phi_y < \frac{1}{\varphi}$ and $1 < \phi_\pi < 1 + \frac{\lambda}{\gamma\varphi}$. The characteristic polynomial of $(\boldsymbol{I} - \boldsymbol{B\beta}^2)^{-1}(\boldsymbol{B} - \boldsymbol{I})$ is given by $h(\nu) = \nu^2 - c_1\nu + c_2$, where

$$
\begin{aligned}
c_1 &= \frac{1}{h(1)}[-(1 - \lambda)(1 - \beta_1^2) - \gamma\varphi(\phi_\pi - 1)(1 + \beta_2^2) - \varphi\phi_y(1 + \beta_1^2) + \lambda\varphi\phi_y(\beta_1^2 + \beta_2^2)], \\
&\le \frac{1}{h(1)}[-\gamma\varphi(\phi_\pi - 1)(1 + \beta_2^2) - \varphi\phi_y(1 + \beta_1^2) + \lambda\varphi\phi_y(1 + \beta_1^2)] < 0 \\
c_2 &= \frac{\varphi}{h(1)}[\gamma(\phi_\pi - 1) + (1 - \lambda)\phi_y] > 0,
\end{aligned}
$$

23

where here $h(1)$ is given in (A.1). Therefore, based on the *Routh-Hurwitz criterion theorem* (see Brock and Malliaris (1989)), both eigenvalues of $(\boldsymbol{I} - \boldsymbol{B}\beta^2)^{-1}(\boldsymbol{B} - \boldsymbol{I})$ have negative real parts. Then following the same ideas of Propositions 1 and 2, we obtain Corollary 1 on the existence and stability of BLE under the forward looking interest rate rule.

# B   Proof of Corollary 2

Under the lagged interest rate rule, the characteristic polynomial of $\boldsymbol{A} + \boldsymbol{B}\beta^2$ is given by $h(\nu) = \nu^2 + c_1\nu + c_2$, where

$$c_1 = -[-\varphi\phi_y + \beta_1^2 - \gamma\varphi\phi_\pi + (\gamma\varphi + \lambda)\beta_2^2], \quad c_2 = (-\varphi\phi_y + \beta_1^2)\lambda\beta_2^2.$$

Based on our assumption $\phi_y < \frac{1}{\varphi}$ and $1 < \phi_\pi < \frac{1-\varphi\phi_y}{\gamma\varphi}$, it is easy to see $h(-1) = (1 - \varphi\phi_y - \gamma\varphi\phi_\pi) + \beta_1^2(1 + \lambda\beta_2^2) + (\gamma\varphi + \lambda(1 - \varphi\phi_y))\beta_2^2 > 0$ and $|h(0)| < 1$ for any $\beta_i \in [-1, 1]$. Furthermore

$$h(1) = (1 - \beta_1^2)(1 - \lambda\beta_2^2) + \varphi\phi_y(1 - \lambda\beta_2^2) + \gamma\varphi(\phi_\pi - \beta_2^2) > 0. \tag{B.1}$$

In addition, for the stability of BLE, direct computations suggest that we need both eigenvalues of $(\boldsymbol{I} - \boldsymbol{A} - \boldsymbol{B}\beta^2)^{-1}(\boldsymbol{A} + \boldsymbol{B} - \boldsymbol{I})$ have negative real parts if $\phi_y < \frac{1}{\varphi}$ and $1 < \phi_\pi < \frac{1-\varphi\phi_y}{\gamma\varphi}$. The characteristic polynomial of $(\boldsymbol{I} - \boldsymbol{A} - \boldsymbol{B}\beta^2)^{-1}(\boldsymbol{A} + \boldsymbol{B} - \boldsymbol{I})$ is given by $h(\nu) = \nu^2 - c_1\nu + c_2$, where

$$\begin{aligned}
c_1 &= \frac{1}{h(1)}[-(1-\lambda)(1-\beta_1^2) - (2 - \lambda(1+\beta_2^2))\varphi\phi_y - \gamma\varphi(2\phi_\pi - (1+\beta_2^2))] < 0, \\
c_2 &= \frac{\varphi}{h(1)}[\gamma(\phi_\pi - 1) + (1-\lambda)\phi_y] > 0,
\end{aligned}$$

where here $h(1)$ is given in (B.1).